Transmissive flexoelectro-optic liquid crystal optical phase modulator with 2π modulation

Cite as: AIP Advances **10**, 055011 (2020); https://doi.org/10.1063/5.0009630
Submitted: 01 April 2020 . Accepted: 22 April 2020 . Published Online: 08 May 2020

Xiuze Wang, Julian A. J. Fells, Taimoor Ali, Jia-De Lin, Chris Welch, Georg H. Mehl, Timothy D. Wilkinson, Martin J. Booth, Stephen M. Morris, and Steve J. Elston

Transmissive flexoelectro-optic liquid crystal optical phase modulator with 2π modulation

Cite as: AIP Advances 10, 055011 (2020); doi: 10.1063/5.0009630
Submitted: 1 April 2020 • Accepted: 22 April 2020 •
Published Online: 8 May 2020

Xiuze Wang,[1] Julian A. J. Fells,[1] Taimoor Ali,[1] Jia-De Lin,[1,2] Chris Welch,[3] Georg H. Mehl,[3] Timothy D. Wilkinson,[4] Martin J. Booth,[1] Stephen M. Morris,[1,a)] and Steve J. Elston[1]

AFFILIATIONS

[1]Department of Engineering Science, University of Oxford, Parks Road, Oxford OX1 3PJ, United Kingdom
[2]Department of Opto-Electronic Engineering, National Dong Hwa University, Hualien 974, Taiwan
[3]Department of Chemistry, University of Hull, Hull HU6 7RX, United Kingdom
[4]Department of Engineering, University of Cambridge, 9 JJ Thomson Avenue, Cambridge CB3 0FA, United Kingdom

[a)]**Author to whom correspondence should be addressed:** stephen.morris@eng.ox.ac.uk

ABSTRACT

In this paper, we demonstrate analog phase modulation in a transmissive configuration using the flexoelectro-optic effect in short-pitch chiral nematic liquid crystal (LC) devices. Two different modes are considered, both of which are shown to generate full 2π phase modulation at 1 kHz switching frequency. The first configuration that is considered consists of a half-wave plate that is placed between two flexoelectro-optic LC devices that are subjected to electric fields that are applied in phase. Second, we demonstrate that a similar phase modulation response can be observed by removing the half-wave plate and subjecting the two flexoelectro-optic LC devices to electric fields whereby the polarities are out of phase. Both configurations demonstrated herein are promising for the development of next-generation LC spatial light modulators, particularly when reflective geometries are challenging or impractical.

I. INTRODUCTION

It is well-known that liquid crystals (LCs) have been successfully deployed in compact spatial light modulator technologies. The exact nature in which the optical phase is altered with the application of voltage depends on the LC mesophase that is employed as the electro-active layer. As an example, nematic LCs can provide multi-level phase control, but due to the relatively thick layers, the response speed can be quite slow, limiting the frequency to <100 Hz.[1–3] Moreover, the response time increases at longer wavelengths. Faster response times are desirable for applications such as beamsteering, microscopy, and micromachining,[4–6] and toward this end, chiral smectic C LCs have been used to generate fast phase modulation, but they cannot typically offer analog phase modulation.[7–9]

Different approaches have been proposed to overcome the inherent limits in each technology; for example, the response time can be reduced in nematic LC devices by increasing the electric field amplitude that is applied across the LC layer, but this comes at the expense of a high driving voltage, which is generally not favorable.[10–13] In addition, some research teams have created a polymer network within the bulk to encourage the LC to relax more rapidly by exploiting the increased anchoring imposed by the network. For instance, a polymer network-based LC light modulator with sub-millisecond response time has been proposed, albeit at infrared wavelengths.[12,14] For visible wavelengths, the trade-off is often the speed of the response at the cost of increased driving voltages and unwanted light scattering. Alternatively, West and co-workers have introduced the concept of using stressed LCs for phase modulation demonstrating rise and decay times of 75 μs and 793 μs, respectively.[3] The downside, however, was that the drive voltage was found to be rather high of the order of 160 Vrms. Impressively, Yan and co-workers have developed a phase modulator that possesses the simultaneous properties of analog modulation, low driving voltage, and polarization-independence, but in this case, the response time for the device was found to be the compromise, being of the order of 2 ms.[2] Despite all of these notable advances, there is still a

need to develop a fast response and low driving voltage analog phase modulator.

In our previous work, we have demonstrated a reflective phase modulator based upon the flexoelectro-optic effect in chiral nematic LCs.[15,16] Briefly, the concept is based on the effect of passing circularly polarized light through a rotatable half-wave plate. In this case, the electrically rotatable half-wave plate is an LC layer that exhibits flexoelectro-optic switching.[17–20] In practice, phase modulation can be realized using our proposed technology by passing linearly polarized light through a quarter-wave plate followed by a chiral nematic LC, aligned in the uniform lying helix (ULH) geometry, and then through a second quarter-wave plate to convert the circularly polarized light back to linear polarization. The range of phase modulation available depends on the angle through which the optic axis of the LC layer can be rotated electrically and is found to be equal to twice the switching angle. Accordingly, flexoelectro-optic devices that can exhibit ±45° switching result in a phase modulation of ±π/2 (i.e., a π phase range).

It has been shown in the previous work that a reflective geometry comprising a flexoelectro-optic LC device placed between two quarter-wave plates in combination with a mirror (or by removing the second quarter-wave plate and replacing the mirror with a chiral reflector) can result in a full 2π phase range with a fast switching frame rate of 1 kHz and low residual amplitude modulation.[15,16] However, for some practical applications, a reflective geometry is not always desirable or feasible.[21] Therefore, in the work presented here, we show two different transmissive phase modulation schemes that could be used to generate a 2π phase range by placing two flexoelectro-optic LC devices in series. The first configuration that is considered consists of two LC devices that are separated by a half-wave plate, and they are switched in the same direction by applying the same bipolar electric field to both devices. The second configuration demonstrated comprises two flexoelectro-optic LC devices for which the optic axes are switched in the opposite direction to one another by applying electric fields to each layer that are of the opposite polarity. In the latter case, no additional half-wave plate is needed.

II. SIMULATIONS

The Jones matrix method[22] has been used in this work to model the optical behavior of the two different configurations of transmissive phase modulators. A schematic of the basic, single LC layer device configuration is shown in Fig. 1. The incident light is converted into circularly polarized light through the combination of a polarizer and a quarter-wave plate, which then passes through a flexoelectro-optic chiral nematic LC device that is aligned in the ULH geometry. The thickness of the LC layer was chosen to provide a half-wave retardance at the wavelength of interest (i.e., λ = 633 nm). Finally, the transmitted light then passes through a second quarter wave plate. Assuming that all the components are ideal, the phase modulation that could be achieved using this configuration ranges from 0 to π, depending upon the deflection of the optic axis and the magnitude of the applied electric field.

The linear polarizer and quarter-wave plate are readily modeled, and the LC can be considered as a wave plate with an optic axis that is in a plane normal to the incident beam. The optical field at the

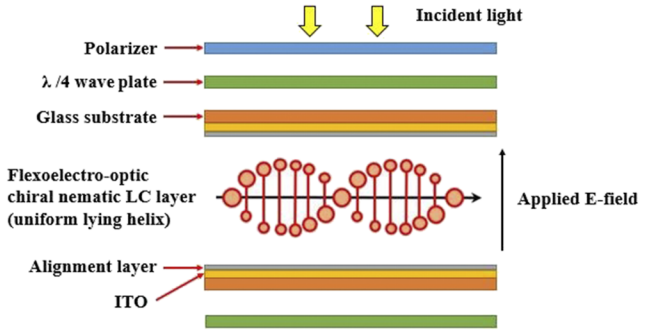

FIG. 1. Illustration of the LC phase modulator configuration containing a linear polarizer, a flexoelectro-optic chiral nematic LC layer in the ULH mode (an electrically tunable half-wave plate), and two quarter-wave plates. The optic axis of the LC layer is parallel to the substrates (horizontal).

output of the device, E_{out}, for the basic single LC layer configuration (i.e., polarizer, quarter-wave plate, LC layer, quarter-wave plate), is given by

$$E_{out} = \mathbf{Q}_2\left(\frac{\pi}{4}\right)\mathbf{D}(\varphi)\mathbf{Q}_1\left(\frac{\pi}{4}\right)\mathbf{P}E_{in}, \tag{1}$$

where $\mathbf{D}(\varphi)$ is the Jones matrix of an LC layer with a retardance, δ, and an optic axis that is oriented at an angle, φ, horizontal to the plane of the device. $\mathbf{Q}_1\left(\frac{\pi}{4}\right)$ and $\mathbf{Q}_2\left(\frac{\pi}{4}\right)$ are the Jones matrices for quarter-wave plates at π/4 to the vertical direction in the lab frame, E_{in} is the Jones vector at the input, and $\mathbf{P}$ is a vertically aligned linear polarizer.[23] Multiplying out the terms in Eq. (1), and assuming that all components are ideal (with the LC layer forming a perfect half-wave plate), leads to

$$E_{out} = E_{in}e^{\pm 2i\varphi}, \tag{2}$$

which demonstrates the dependence of the phase on the switching angle of the optic axis of the LC layer. In other words, the phase range equates to twice the switching angle.

Figures 2(a) and 2(b) show the configurations of the two transmissive phase modulators that comprised two LC layers, and they are based on the fundamental device configuration shown in Fig. 1. Both configurations include two LC devices, two quarter-wave plates, and a polarizer, but as mentioned previously, a half-wave plate is placed in between the two LC cells in configuration I [Fig. 2(a)] and the electric field applied to the two LC layers is in the same direction. For configuration II, the need for an additional half-wave plate is negated as the electric fields are applied in opposite directions.

The optical output field, E_{out}, for configurations I and II is given, respectively, by

$$E_{out} = \mathbf{Q}_2\left(\frac{\pi}{4}\right)\mathbf{D}(\varphi)\mathbf{H}_1\left(\frac{\pi}{2}\right)\mathbf{D}(\varphi)\mathbf{Q}_1\left(\frac{\pi}{4}\right)\mathbf{P}E_{in}, \tag{3}$$

$$E_{out} = \mathbf{Q}_2\left(\frac{\pi}{4}\right)\mathbf{D}(-\varphi)\mathbf{D}(\varphi)\mathbf{Q}_1\left(\frac{\pi}{4}\right)\mathbf{P}E_{in}. \tag{4}$$

Note that in Eq. (4), the angles of the optic axis in the LC layers are of opposite signs because the electric fields are of the opposite polarity

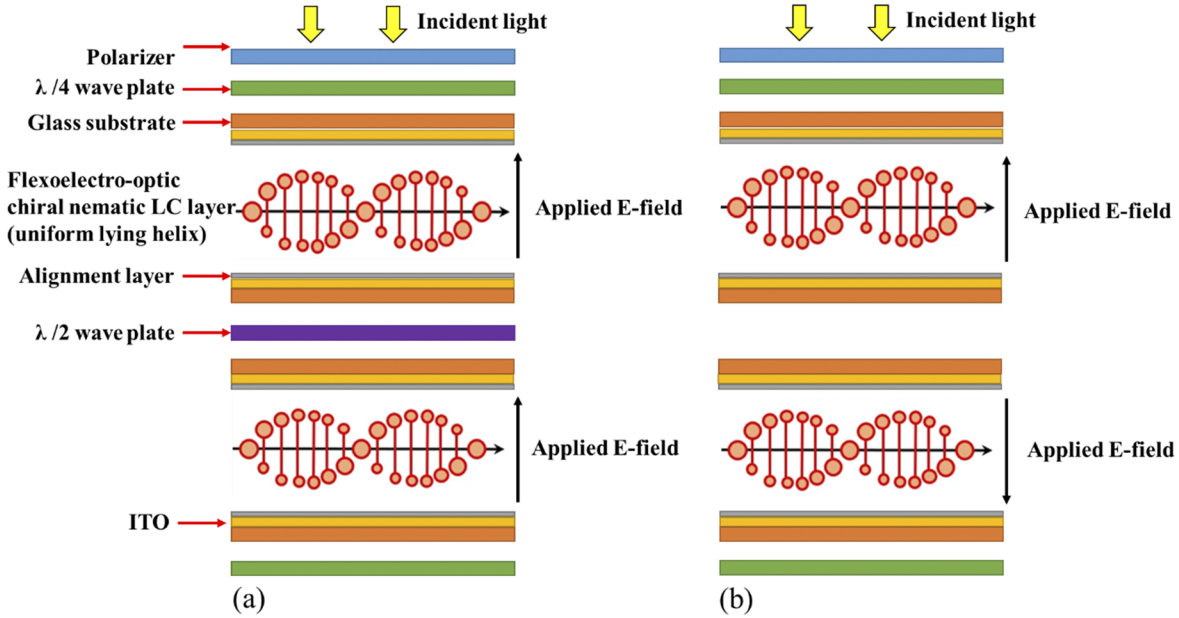

FIG. 2. Illustration of the two configurations of transmissive LC phase modulators considered in this work. (a) Configuration I comprises two flexoelectro-optic chiral nematic LC cells in the ULH geometry, two quarter-wave plates, a half-wave plate, and electric fields that are applied to both LC cells that are in-phase. (b) Configuration II consists of two flexoelectro-optic chiral nematic LC cells in the ULH geometry and two quarter-wave plates. The electric fields applied to the LC cells are of the opposite polarity.

and there is no half-wave plate in the middle of the two LC devices ($\mathbf{H}_1$). Multiplying out the terms in Eqs. (3) and (4) (assuming that all components are ideal) leads to the following result:

$$E_{\text{out}} = E_{\text{in}} e^{+4i\varphi}. \tag{5}$$

From Eq. (5), it can be seen that a switching angle of φ will result in a 4φ phase modulation. For our study, the switching angle of our LC layer is within the range of 90° (i.e., a tilt angle of the optic axis in the ULH device of ±45°); hence, a phase modulation of ±π can be obtained (i.e., a 2π phase range).

Figure 3 illustrates the results from simulations based on Eqs. (3)–(5). For the simulations, the LC and quarter-wave plates are assumed to be ideal (e.g., the LC behaves as an ideal half-wave plate). When all the components are ideal, the basic configuration generates a phase modulation that is twice that of the switching angle of the optic axis of the flexoelectro-optic LC layers. On the other hand, configurations I and II lead to a phase modulation that is a multiple of four of the switching angle of the flexoelectro-optic LC layers as expected. The results show that when all the components in the system are assumed to be ideal, the single flexoelectro-optic device configuration is limited to a phase range of π for a switching angle of ±45°, whereas for configurations I and II, a 2π phase range is obtained for the same switching angle of the LC layers. As shown, no amplitude variation is observed when all the components in each system are considered to be ideal.

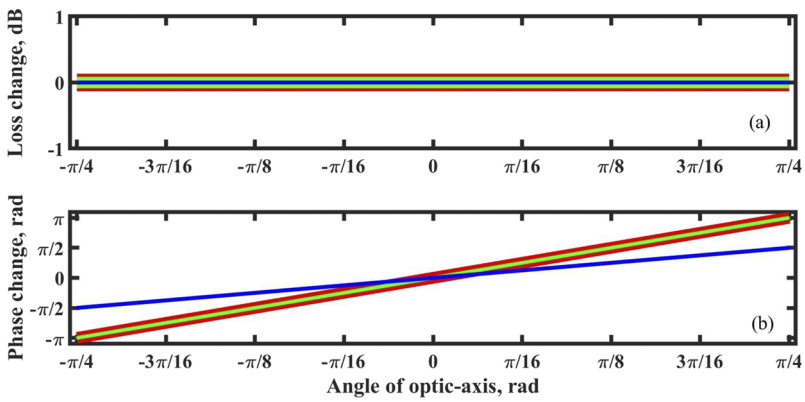

FIG. 3. Results from simulations using Eqs. (3)–(5) for the basic device stack consisting of only one LC layer along with the two device configurations shown in Fig. 2. Both the loss change (a) and the phase change (b) are presented as a function of the tilt angle of the optic axis of the flexoelectro-optic LC layers. The blue lines in both plots are the results for the single transmissive device (consisting of a single LC layer, as shown in Fig. 1), whereas the green line represents configuration I [Fig. 2(a)] and the red thick line represents the response for configuration II [Fig. 2(b)].

III. EXPERIMENTAL

The device configurations in Figs. 1 and 2 were investigated experimentally using a Mach–Zehnder interferometer arranged as shown in Fig. 4. In this case, the device under test (DUT) corresponds to either the basic single flexoelectro-optic device configuration or configurations I or II. Light from a helium–neon laser at 632.8 nm (Uniphase 1125P) was passed through a linear polarizer (vertical in the lab frame) to a 50:50 non-polarizing beam splitter (Newport 05BC16NP) in order to divide the beam into separate arms. For the first arm, 50% of the light was directed to a mirror before it was incident on the second beam splitter (BS2, Thorlabs CM13) where it combined with the light that had propagated through the second arm of the interferometer (which contained one of the LC phase modulator configurations). After passing through the first beam splitter (BS1), the light propagating along the second arm of the interferometer then passed through a linear polarizer before entering the DUT.

The configurations for each DUT are shown explicitly in Fig. 5. In all three cases, the outer components of the DUT are the quarter-wave plates. For the basic, single flexoelectro-optic device [Fig. 5(a)], a pair of lenses (L1 and L2) were used to ensure that the light only passed through a mono-domain region of the LC device (which were typically 50–100 μm^2 in size). Figure 5(b) shows the arrangement for experimentally testing configuration I [Fig. 2(a)], which is similar to the basic configuration except with the addition of the extra LC device and a half-wave plate (H), which are introduced into the modulation arm to produce a 0–2π phase modulation range in accordance with the results obtained from simulations (Fig. 3). In this case, instead of using just a pair of lenses, an additional lens (L2) is added between the two LC devices to form a three lens (2f–f–2f) system so that the light can be appropriately focused onto mono-domain regions within the two LC layers. Similarly, Fig. 5(c) shows the arrangement for testing configuration II. Here, the electric field applied to the second LC layer is of the opposite polarity to the electric field applied to the first LC layer, which negates the use of the half-wave plate (H).

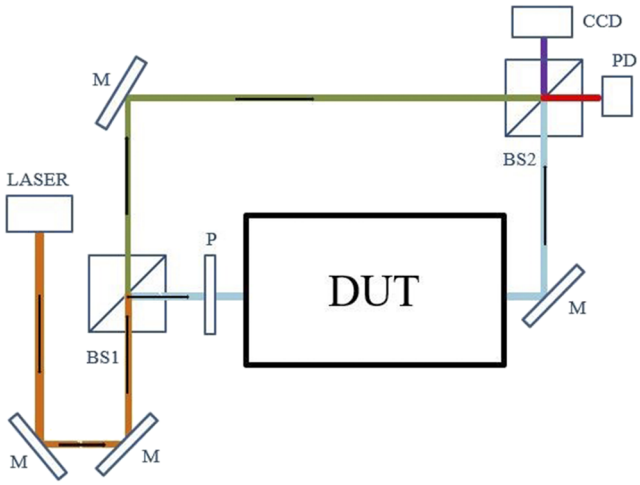

FIG. 4. The Mach–Zehnder interferometer used to measure each device under test (DUT), which represents either the basic single LC device (Fig. 1) or the two LC device configurations (Fig. 2). The remaining components are M, mirror; BS1, BS2, beam splitters; CCD camera; and PD, photodiode.

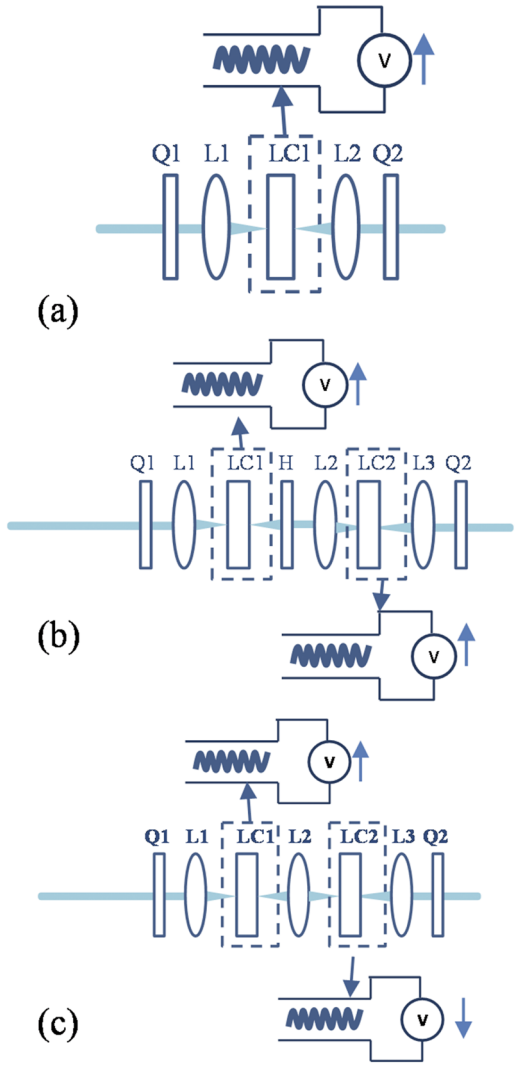

FIG. 5. Experimental arrangement of the three different DUTs inserted in the Mach–Zehnder interferometer shown in Fig. 4. (a) Basic configuration with one LC layer, (b) configuration I, and (c) configuration II (H, half-wave plate; Q1 and Q2, quarter-wave plates; L1, L2, and L3, lenses; and LC1 and LC2, phase modulation devices).

After passing through the DUT, light from both arms of the interferometer is combined at the beam splitter to generate an interference pattern. The phase and amplitude responses were subsequently recorded by using a CCD camera (Thorlabs DCU224C, 1280 × 1024, 8-bit color) and a photodiode, respectively. The drive signal for the LC device was set as a 1 kHz square-wave with a controllable amplitude level, and the camera was set to an exposure time of 100 μs so as to record the change observed in the interference fringes when the amplitude of the electric field applied across the LC device was altered.

For this study, the LC mixture that was used throughout consisted of the bimesogen (dimer) CB7CB [4′,4′-(heptane-1,7-diyl)bis(([1′,1″-biphenyl]-4″-carbo-nitrile))] dispersed with 3 wt. % of the high twisting power chiral dopant, BDH1281 (Merck KGaA). This bimesogen was chosen as it has been shown to exhibit large flexoelectro-optic switching in previous work.[24–26] The chiral nematic mixture was filled into a nominally 5 μm-thick Instec cell (corresponding to a half-wave plate condition) with antiparallel rubbed polyimide alignment layers and indium tin oxide electrodes. The LC mixture was found to exhibit a right-handed chiral nematic phase between 106 °C and 113 °C (on heating) with a pitch of ≈400 nm. To obtain a ULH alignment, the cell was first heated to 120 °C (above the clearing temperature) and then cooled down in the presence of a 1 kHz, ±30 V square-wave signal applied to the cell electrodes. This alignment process was found to result in monodomains that were typically 150 × 150 μm^2 in size, in accordance with the results presented in a previous study for a comparable LC layer.[27] All subsequent measurements were carried out with the device in the chiral nematic phase at a temperature of 108 °C. At this temperature, the switching time (10%–90% response time) of the device was found to be ≈160 μs. Each LC device was mounted on a temperature-controlled hot-stage, and an electric field was applied using an arbitrary function generator (Wavetek 395) and a voltage amplifier (FLC Electronics F10AD).

IV. RESULTS AND DISCUSSION

Images of the interference fringes recorded by using the CCD camera of the interferometer for the basic configuration, configuration I, and configuration II are shown in Fig. 6. Figure 6(a) shows five different images of the interference fringes, each representing a phase modulation state corresponding to a specific voltage applied to the single LC layer. For this configuration, the shift in the fringes corresponding to a π phase change is found to occur for ±34 V (6.9 V/μm). Alternatively, for configurations I and II, shown in Figs. 6(b) and 6(c), respectively, a 2π phase shift is observed for an applied voltage of ±34 V.

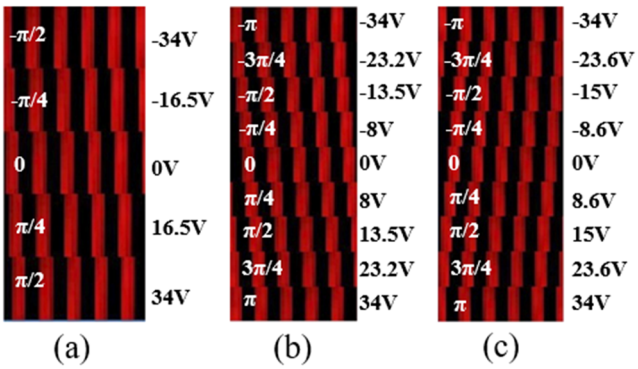

FIG. 6. Images recorded on the CCD of the Mach–Zehnder interferometer for the basic device configuration and the two configurations I and II. (a) Results for the basic, single LC device configuration. Nine images for (b) configuration I and (c) configuration II. These are shown for modulated phase angles at π/4 intervals.

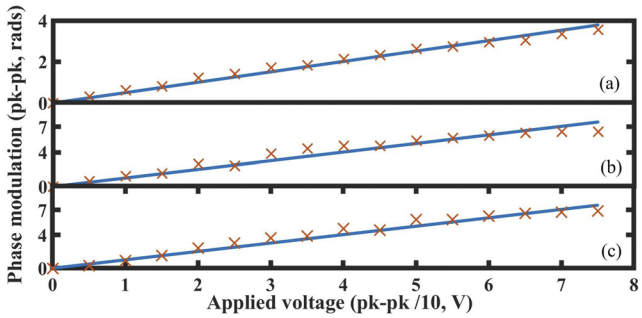

FIG. 7. Phase modulation extracted from the interference fringes in Fig. 6 plotted as a function of the applied voltage for (a) the basic (single LC layer) configuration, (b) configuration I, and (c) configuration II. Lines of the best fit to the experimental data (shown in blue) are also presented.

Figure 7 shows the results for the optical phase modulation of the three configurations as a function of the voltage applied to the LC layer(s). These are found to be in good agreement with the simulations in Fig. 3 in that both configurations I and II exhibit full 2π phase modulation, whereas the basic single LC device shows a phase modulation that is about π for a switching angle of ±45°. In order to show that some of the configurations can provide greater than 2π (6.3 rad) phase range, the applied voltage was varied up to ±37.5 V (7.6 V/μm) and the range was found to be almost 2.2π (6.9 rad). From this figure, it can be seen that in all cases, the phase change as a function of voltage appears to follow a roughly linear behavior across the voltage range considered here, which again is in good agreement with the simulation results shown in Fig. 3. It should be noted that the intensity variation measured by using the photodiode was found to be very small in each case.

For the basic single LC configuration [Fig. 7(a)], the slight deviation from the linear dependence seen in the optical phase behavior is believed to come from (i) the flexoelectro-optic tilt angle in the ULH device not being perfectly linear with applied voltage and (ii) small drifts in the environmental temperature and corresponding air currents (caused principally by hot-stage stabilizing the device temperature) leading to small drift errors in the phase extracted from the fringes. For the other two configurations, it can be observed that the deviation from linear dependence is slightly larger than that recorded for the basic configuration: this is because two LC layers are used, which increases the drift errors described previously. Compared with our previous results,[15,16] which achieve a 2π phase modulation with a reflective geometry, the transmissive configurations presented here exhibit a greater deviation from linear dependence. It is expected that the drift caused by the environment is small compared with the nonlinearities introduced by the LC layers.

V. CONCLUSION

In summary, we have presented three different transmissive mode LC optical phase modulators based on the flexoelectro-optic effect of a chiral nematic LC aligned in the ULH geometry. A basic configuration consisting of a single LC layer between quarter-wave

retarders is found to exhibit a phase modulation of π corresponding to a ±45° switching angle of the flexoelectro-optic effect. To achieve full 2π modulation in transmission with flexoelectro-optic devices that exhibit a switching angle of ±45°, an additional LC layer is required. It has been shown that this can be achieved by either adding a half-wave plate in between two LC layers when the electric field applied to both LC layers is the same or applying electric fields of opposite polarity, avoiding the need for an additional half-wave plate.

Both configurations are investigated using simulations involving Jones matrices and are found to be consistent with our experimental results when the chiral nematic LC layers exhibit ±45° switching angles. This is achieved using LC layers that consist of the bimesogen CBC7CB doped with a 3 wt. % chiral dopant, which is subjected to an applied electric field of 6 V/μm at a temperature of 108 °C. These configurations have potential in terms of the development of spatial light modulator technology, enabling full 2π phase modulation with low-intensity modulation to be achieved when transmissive devices and geometries are required.

ACKNOWLEDGMENTS

The authors gratefully acknowledge the Engineering and Physical Sciences Research Council (UK) for financial support through Grant Nos. EP/M017923/1, EP/M015726/1, and EP/M016218/1 as well as the European Space Agency for support through Contract No. 4000125232/18/NL/AR/zk. T.A. would like to thank the Punjab Educational Endowment Fund (Pakistan) and the Vicky Noon Education Foundation for financial support during his graduate studies.

DATA AVAILABILITY

The data that support the findings of this study are available from the corresponding author upon reasonable request.

REFERENCES

[1] L. Grigory, B. Stefanie, E. Philip, H. Daniel, and N. Gunther, Proc. SPIE **10335**, 103351B (2017).
[2] K. Yan, Q. Guo, F. Wu, J. Sun, H. Zhao, and H. Kwok, Opt. Express **27**, 9925 (2019).
[3] J. L. West, G. Q. Zhang, A. Glushchenko, and Y. Reznikov, Appl. Phys. Lett. **86**, 031111 (2005).
[4] J. M. Bueno, J. Opt. A: Pure Appl. Opt. **2**, 216 (2000).
[5] H. Ren, Y.-H. Fan, Y.-H. Lin, and S.-T. Wu, Opt. Commun. **247**, 101 (2005).
[6] C.-Y. Liu and L.-W. Chen, Opt. Express **12**, 2616 (2004).
[7] T. Drabik, MRS Proc. **392**, 111 (1995).
[8] N. Collings, J. Gourlay, D. G. Vass, H. J. White, C. Stace, and G. M. Proudley, Appl. Opt. **34**, 5928 (1995).
[9] S. Broomfield, M. Neil, and E. Paige, Appl. Opt. **34**, 6652 (1995).
[10] J. Hahn, H. Kim, Y. Lim, G. Park, and B. Lee, Opt. Express **16**, 12372 (2008).
[11] H. Xianyu, S.-T. Wu, and C.-L. Lin, Liq. Cryst. **36**, 717 (2009).
[12] J. Sun, Y. Chen, and S.-T. Wu, Opt. Express **20**, 20124 (2012).
[13] F. Peng, D. Xu, H. Chen, and S.-T. Wu, Opt. Express **23**, 2361 (2015).
[14] Y.-H. Fan, Y.-H. Lin, H. Ren, S. Gauza, and S.-T. Wu, Appl. Phys. Lett. **84**, 1233 (2004).
[15] J. A. J. Fells, X. Wang, S. J. Elston, C. Welch, G. H. Mehl, M. J. Booth, and S. M. Morris, Opt. Lett. **43**, 4362 (2018).
[16] X. Wang, J. A. J. Fells, W. C. Yip, T. Ali, J.-D. Lin, C. Welch, G. H. Mehl, M. J. Booth, T. D. Wilkinson, S. M. Morris, and S. J. Elston, Sci. Rep. **9**, 7016 (2019).
[17] J. S. Patel and R. B. Meyer, Phys. Rev. Lett. **58**, 1538 (1987).
[18] P. Rudquist, L. Komitov, and S. T. Lagerwall, Phys. Rev. E **50**, 4735 (1994).
[19] P. Rudquist, L. Komitov, and S. T. Lagerwall, Liq. Cryst. **24**, 329 (1998).
[20] P. Rudquist, T. Carlsson, L. Komitov, and S. T. Lagerwall, Liq. Cryst. **22**, 445 (1997).
[21] M. Choi and J. Choi, Opt. Express **25**, 22253 (2017).
[22] R. C. Jones, J. Opt. Soc. Am. **31**, 488 (1941).
[23] J. J. Gill and E. Bernabeu, Optik **76**, 67 (1987).
[24] A. Varanytsia and L. C. Chien, "Giant flexoelectro-optic effect with liquid crystal dimer CB7CB," Sci. Rep. **7**, 41333 (2017).
[25] A. Varanytsia and L.-C. Chien, J. Appl. Phys. **119**, 014502 (2016).
[26] V. Joshi, K.-H. Chang, A. Varanytsia, D. A. Paterson, J. M. D. Storey, C. T. Imrie, and L.-C. Chien, Adv. Opt. Mater. **6**, 1800013 (2018).
[27] J. A. J. Fells, C. Welch, W. C. Yip, S. J. Elston, M. J. Booth, G. H. Mehl, T. D. Wilkinson, and S. M. Morris, Opt. Express **27**, 15184 (2019).